

Improved Encoding of Wavelet Coefficients Extracted from Multispectral and Hyperspectral Image Data

Vishnu Makkapati

Honeywell Software Solutions Lab
151/1, Doraisanipalya, Bannerghatta Road
Bangalore - 560 076, India
vishnu.makkapati@honeywell.com

Rajeev Kumar

Computer Science & Engineering Department
Indian Institute of Technology
Kharagpur - 721 302, India
rkumar@cse.iitkgp.ernet.in

Abstract

An effective and lossy compression technique for multispectral and hyperspectral image data minimizes both the spatial and spectral correlations while preserving the spectral characteristics of the data. In this paper, we use two-dimensional wavelet transform and propose an encoding technique for wavelet coefficients. We use Kronecker-Product Gain-Shape Vector Quantization coupled with the generalized BFOS for obtaining an optimal bit-rate. Results are presented for multispectral and hyperspectral data taken from different sensors in different bands. It is shown that for a given bit-rate, the image quality is superior than other techniques designed for such image data.

1. Introduction

Remotely sensed earth-observation data is finding increasing applications in land-use management, meteorology, geology and military surveillance. Airborne and spaceborne sensors acquire data in many spectral bands with high spatial and radiometric resolutions. If the image is composed of a few spectral bands it is called multispectral while the image consisting of many tens of bands is called hyperspectral. Hyperspectral images provide much *richer spectral* information. (In rest of the paper, at *many* places but section 4, we use the term multispectral to mean both multispectral and hyperspectral). In either of the cases, the data occupies large space and compression of the data is always desired. Image compression algorithms for traditional (a single spectral band) images take into account the psychovisual features both in space and frequency domain and exploit the spatial correlation along with the statistical redundancy. Almost all practically used algorithms adopt a *quantization* stage which makes the algorithms lossy and thus achieve a desired compression ratio.

Multispectral data exhibits a large spectral correlation. The compression algorithms minimize spectral correlation too in a *lossy* manner to achieve larger compression gain.

However, usages of multispectral data are dependent mostly on rich spectral information contained in such images. So a practical algorithm for multispectral data should preserve spectral characteristics of the data while working in a lossy manner and maximize the gain.

Many techniques have been proposed for multispectral image data. Almost all techniques minimize *intra-band* and *inter-band* correlation, some do in a single step and others in a two-step transformation followed by an encoding scheme to eliminate the statistical redundancy or to give a desired bit-rate. The main issue is that the algorithm should be *lossy*, encoding scheme *may be sub-optimal* in some respect but it should *preserve* the spectral characteristics of the data and be of *lesser* algorithmic complexity.

In this paper, we present an algorithm which works with wavelet transform [3] and encodes the coefficients using gain-shape vector quantization [6] such that we get superior image quality for a given bit-rate. In doing so, we make an assumption that spectral correlation exists in the biorthogonal subclasses of multispectral/hyperspectral images, we prove this assumption empirically in the later part of this paper. We make use of the Generalized BFOS algorithm [16] to allocate bits among different subbands. The remainder of the paper is organized as follows. In section 2, we briefly review the existing approaches and the performance metrics. We describe, in section 3, our approach which encodes wavelet coefficients extracted from multispectral images. We present results, in section 4, obtained from multispectral and hyperspectral data acquired from different sensors along with a brief analysis. We compare the results obtained with our technique to those which were recently reported. Finally, we draw conclusions in section 5.

2. Review of Existing Approaches

In recent years, many coding techniques have been proposed for multispectral and hyperspectral data. In general, almost all the approaches adopt a two stage process, first, the data is transformed into some other domain and/or rep-

resented by the indices of the codebook, followed by an encoding of the transformed coefficients or the codebook indices. In the following subsections, we briefly describe the approaches available in literature along with a critical analysis. Then we comment upon the performance of the algorithms.

2.1. Spatial and Spectral Correlation

The first stage is to minimize the intraband and interband correlation or to make use of the correlation so as to reduce the data. Most commonly adopted approaches rely on the transformed techniques [10] and/or the use of vector quantization [12].

Most of the algorithms exploit spectral and spatial correlations independently, assuming that both types of correlations are independent. Karhunen-Loeve transform (KLT) [8] is commonly used for multispectral images for feature selection, classification and spectral decorrelation. Discrete cosine transform (DCT) is used practically in almost all single band image and video compression techniques, e.g., JPEG and MPEG, to decorrelate spectral redundancy. Wavelet Transform has been proven to be very effective and gaining popularity over DCT transform. A 2-D Discrete Wavelet transform (DWT) obtains a set of biorthogonal subclasses of images by decomposing the image at different scales using a pyramidal algorithm architecture, and enables high compression bit-rates through the proper use of bit-allocation in the subimages. (For details of wavelet theory - see [15]). DWT extracts not only frequency information but also spatial information, and can be adapted to progressive transmission with low-bit rate [3].

Many authors used KLT to decorrelate spectral redundancy, and DCT or DWT to decorrelate spatial redundancy. For example, Saghri & Tescher [18] and Lee [14] used KLT followed by a 2-D DCT, and Epstein [9] and Amato et al. [2] used KLT and DWT. Some others used DCT followed by an interband predictive coding [1]. However, interband relationship is highly *non-linear*, better to say un-predictive in the absence of *a priori* knowledge of the image itself, so predictive approaches would not work well with a natural image. However, transform based approaches have been used by most of the researchers in some combination or the other.

Instead of applying a hybrid strategy, one for spatial and another for spectral, Abousleman et al. [1] applied a 3-D DCT on $8 \times 8 \times 8$ datacubes of hyperspectral images. Similarly, Tseng et al. [20] used a 3-D DWT to simultaneously decorrelate the spectral and spatial information, and extract the most representative contents in wavelet coefficients. They applied a separable 3-D DWT to hyperspectral data resulting in wavelet coefficients which were encoded using the entropy coding after an optimal scalar quantization stage. Tseng et al. used AVIRIS images and performed

compression with various combination of wavelet banks, transformation levels and quantization levels, and achieved interesting results. However, their technique is not suitable to multispectral data because of a few spectral bands [19].

Among the non-transformed approaches are the spectral classification based and the vector quantization based techniques. Gelli & Poggi [11] used spectral classification as the first stage. Many researchers made use of some or the other variants of Vector Quantization (VQ). VQ encodes a sequence of samples rather than encoding a sample and automatically exploits both linear and non-linear dependencies. It is shown that VQ is optimal among block coding techniques, and that all transform coding techniques can be taken as a special case of VQ with some constraints [12]. In VQ, encoding is performed by approximating a sequence to be coded by a vector belonging to a codebook. Creation of a straight and unconstrained codebook is a computationally intensive and the complexity grows exponentially with the block size; codebook creation is an NP-problem. So one uses a small block size; many greedy algorithms and the constraints exist in the literature for a practical solution. For example, Lindo-Buzo-Gray (LBG) classification algorithm with mean squared criterion (MSE) is used to create a codebook, this algorithm may converge iteratively to a *locally* optimal codebook [12]. Secondly, it is almost impossible to create a universal codebook which works across all the images.

Researchers used many variants of VQ for multispectral image compression. Aim is to get an efficient and faster algorithm *may be* with some *sub-optimality*. Some used VQ for spatial correlation while others used for spectral information. For example, Baker & Tse [4] used VQ for spectral blocks, and Gupta & Gresho [13] used VQ for spatial blocks and prediction for spectral. Both used smaller block size.

To overcome the limitations of the block-size, some sub-optimal constrained VQ algorithms were proposed which are many times more computationally efficient than the unconstrained VQ. The huge complexity reduction allows one to use much larger blocks and to better exploit the redundancy. Gain-Shape VQ (GSVQ) is one of the most popular algorithms which belongs to the class of product-code VQ in which a VQ is obtained as the Cartesian product of two or more smaller codebooks [17]. Canta & Poggi built upon GSVQ a new encoding scheme for multispectral data. The technique is known as Kronecker-Product Gain-Shape VQ (KRGSVQ) [6] and takes advantage of the characteristics of multispectral data. Their basic assumption is that the shape of a block in a given spatial position does not change significantly from band to band, and only the gain term changes to account for the variations of reflectivity across the spectral bands. They found the technique over hundred times more computationally efficient than unconstrained VQ, and over ten times efficient than direct GSVQ. For a given level of

complexity and a given image quality, they got a compression ratio five times larger than that provided by ordinary VQ.

In place of applying VQ to image data, many researchers applied some or the other variants of VQ to transform coefficients extracted from multispectral data. For example, Vaisey et al. [21] used lattice VQ on wavelet coefficients extracted from multispectral data. They also used Lattice VQ with KLT and compared the results obtained with Lattice VQ in individual combination of KLT and DWT.

In general researchers have used KLT, DCT, DWT and/or some constrained VQ for decorrelating both spatial and spectral information. In this work, we too used the same basic tools but in an unique combination, we use DWT for spatial correlation followed by a constrained VQ which works on coefficients rather than the image data itself.

2.2. Statistical Redundancy & Bit-Allocation

In bit-allocation, a given number of bits is assigned to a set of different sources (e.g., coefficient of wavelet subbands or the indices of multiclass codebooks in VQ) to minimize the overall distortion of the coder. An optimal but simple codec is an entropy coder which allocates bits based on the symbol probabilities and thus eliminates statistical redundancy. In Tseng et al. [20], wavelet coefficients were compressed using an optimal scalar quantizer followed by variable length huffman codes. Tseng et al. reported the results that spectral classification accuracy did not drop in response to an increase in information loss due to quantization and decomposition.

However, from Shanon's rate-distortion theory, coding performance can always be improved with vectors rather than scalars, and it can be further increased with use of larger blocks. (Looking from another angle, number of distortion measures increases with increase in block size. So for a given computational complexity, sub-optimal techniques can often outperform VQ by simply using larger blocks.) For a fixed-rate, each codebook contains the same number of codewords. In a variable bit-rate (VBR), codebook size is varied and variable number of bits are allocated to code-vectors.

Generalized BFOS algorithm is an extension of Breiman, Friedman, Olshen and Stone's pruning algorithm in tree-structured classification and regression [5]. Chou et al. [7] used this algorithm for tree-structured source coding, and Westerink et al. [22] applied in sub-band coding for optimal bit-allocation. Riskin analyzed this algorithm for optimality and algorithm complexity [16].

Since then much work has been done on Gen. BFOS algorithm, and many researchers used this algorithm for optimal bit allocation in variable rate VQ design and subband coding. For example, Vaisey et al. [21] used this algorithm in Lattice VQ design of KLT and DWT coefficients.

2.3. Performance of the Algorithms

Most of the researchers have reported the performance of multispectral data in terms of bit-rate versus SNR/PSNR. Few approximated the algorithmic complexity in terms of the number of operations. Some presented a few of the original and decompressed images for visual comparison. Main purpose of all these results is to evaluate the quality of the decompressed data subjectively and objectively. However, the quantitative SNR/PSNR metrics are too generic because they are averaged over all the pixels. Usually image is most degraded at high frequency components, e.g., edges and discontinuity; this usually demarcates a boundary for spectral classification. A generic nature of SNR/PSNR type of measure serves some purpose but it is not an authoritative measure to evaluate the spectral image quality.

So some researchers (e.g., [6] and [20]) presented results of pixel-to-pixel classification. There are many methods available in literature, e.g. nearest neighbor, maximum likelihood, supervised and unsupervised clustering [8]. All such methods incorporate machine learning, and the performance is governed by many parameters such as the selection of the datasets for training and validation, learning algorithms, convergence criterion and the rate of convergence. This itself is an open problem. Therefore, it is not trivial to have a straight forward metric to quantitatively evaluate the spectral quality.

3. Proposed Algorithm

In this work, we use DWT for multispectral image compression. We make an assumption that spectral correlation exists in wavelet coefficients of multispectral image. We empirically prove this assumption while presenting and discussing the results in section 4. This scheme exploits the spatial and spectral correlation in the biorthogonal subclasses of multispectral image. The proposed scheme consists of two steps. First, all bands of multispectral image are analyzed independently using two-dimensional DWT. Then, the wavelet coefficients are quantized with multiresolution codebook using Kronecker- Product Gain-Shape Vector Quantization (KRGSVQ)[6], and encoded using Generalized BFOS algorithm [16].

3.1. Wavelet Decomposition

We decompose all the bands of multispectral image upto two levels using pyramidal algorithm [3]. The four subbands from analysis with biorthogonal filters in horizontal and vertical directions are LL, LH, HL and HH which represent the low, horizontal, vertical and diagonal resolution sub-images - see Figure 1 where subscript represents the resolution level. The filters used for decomposition are high pass and low pass filters. LH, HL and HH contain finer details of the image while LL contains coarser details. LL and

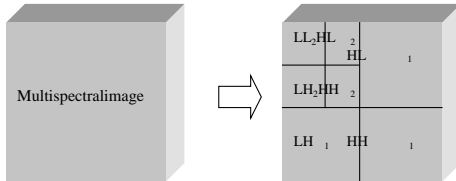


Figure 1: Two level wavelet decomposition.

HH represent the components corresponding to analysis in horizontal and vertical directions with low pass and high pass filters respectively. Hence DWT concentrates maximum signal power into the LL subimage while HH subimage contains least signal power. Such a wavelet decomposition permits the generation of a multiresolution codebook.

3.2. Encoding of Wavelet Coefficients using Gain-Shape Vector Quantization

We use KRGSVQ encoding scheme for quantizing the wavelet coefficients. This technique was proposed by Canta & Poggi [6] for multispectral data. They applied in the spatial domain and we, in this work, use this technique for wavelet coefficients. KRGSVQ relies on the assumption that the shape of a generic spatial block remains the same in all bands while the gain changes to reflect the bands in multispectral image. The gain is vector quantized using a codebook of gains while the shape is vector quantized using a codebook of shapes. The computational overhead due to KRGSVQ is minimal and so makes it suitable for compression of multispectral images.

We make an assumption that the shape of a generic spatial block remains the same even in the biorthogonal subclasses of multispectral image. We encode the subbands using multiresolution gain and shape codebooks for each preferential direction using KRGSVQ. The initial codebooks are generated by choosing the shape and gain codevectors randomly from the representation gain and shape vectors of the subbands of multispectral image.

3.3. Generalized BFOS for Bit-Allocation

We use the generalized BFOS (Gen BFOS) algorithm [16] to allocate bits between different subbands after multiscale decomposition. Gen BFOS assumes that rate-distortion table is available. We calculate the rate-distortion table for the subbands using KRGSVQ by constraining the sum of sizes of shape and gain codebooks. Two kinds of error are associated with KRGSVQ. One is the representation error associated with representing the wavelet coefficients as Kronecker-Product of Gain and Shape. The second error is due to encoding the representation gain and shape vectors with codebooks. We find the convex hull by calculating the slopes due to deallocating more than one bit at a time. Bits

allocated for each direction are distributed between the gain and shape codebooks. We computed the mean square error (MSE) corresponding to all possible combinations of the sizes of gain and shape codebooks that correspond to a specific bit rate and considered the combination that resulted in minimum MSE.

The rate-distortion table (bits per pixel versus MSE) used in BFOS is computed using KRGSVQ. For example, 1 bits per pixel (bpp) is distributed among subbands (e.g., HL_1 , HH_1 , LH_1 , HL_2 , HH_2 and LH_2). The rate-distortion table (0 to 1 bpp) is computed for each of the subbands using KRGSVQ, so six tables are computed which are given as input to Gen BFOS. Now the overall bpp is six instead of one. Gen BFOS deallocates the bpp allocated to subbands till the required rate of 1 bpp is achieved.

4. Experimental Results and Analysis

We carried out a number of experiments with multispectral and hyperspectral data. A few representative results are included here. We considered a square region of 512×512 pixel area for each test image. We use 9/7 biorthogonal filters for decomposing and reconstructing the images [3]. We measured distortion in terms of Peak-Signal-to-Noise-Ratio (PSNR) and Signal-to-Noise-Ratio (SNR). For each of the datasets, approximately 90% of the signal power was concentrated in lower frequency components.

In Figures, the symbols N_g , N_s and bpp represent size of the gain codebook, size of the shape codebook and bits per pixel respectively. For each of the cases, we took a block-size of 4×4 for HH_2 sub-image because of comparatively lower signal content, a choice can always be made between the block-size and the codebook size. We encode LL_2 subimage with the same number of bits as they are in the raw image; this is 8 bpp for IRS and Landsat images and 9 bpp for GER data - see sub-band bit-allocation maps in Figures 2 and 5. Bit-rate is expressed in bits per pixel and should be divided by the number of bands to obtain *bits per pixel per band*. The PSNR corresponding to 0.5 bpp represents the case where all the biorthogonal subclasses except for the low-frequency component are discarded (Figures 3 and 4).

4.1. IRS LISS-III Four-Band Data

First, we applied our technique to IRS LISS-III four spectral band data. We took data of an area near Delhi. Figure 2 shows the bit allocation. The signal content at level 1 is very less. Hence low bit rate is assigned to the wavelet coefficients at resolution level 1. Gain accounts for the band power while shape is invariant across bands. Hence the gain codebook size is smaller than that of the shape codebook for sub-images LH_1 , HL_1 , HH_2 with less signal content while it is greater than the shape codebook for LH_2 and

8 bpp	1.75 bpp $N_g = 70$ $N_i = 58$ Size 2×2	0.5 bpp $N_g = 76$ $N_i = 180$ Size 4×4
1.75 bpp $N_g = 67$ $N_i = 59$ Size 2×2	0.5 bpp $N_g = 59$ $N_i = 61$ Size 4×4	0.5 bpp $N_g = 197$ $N_i = 197$ Size 4×4
0.5 bpp $N_g = 63$ $N_i = 193$ Size 4×4	0 bpp $N_g = 0$ $N_i = 0$ Size 4×4	0.5 bpp $N_g = 0$ $N_i = 0$ Size 4×4

Figure 2: Sub-band bit allocation for IRS image at 1 bpp.

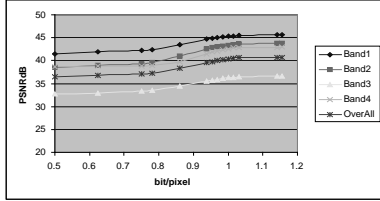


Figure 3: PSNR versus bpp for IRS image.

HL_2 sub-images. HH_1 contains minimal signal and hence is discarded, the other components contain significant image information and are assigned bit rate accordingly. LH_1 and HL_1 contain almost the same signal content and hence are assigned equal bit rate.

Figure 3 represents PSNR versus bits per pixel for this data. Band 2 (power = 3016.17) of IRS image contains less signal power as compared to Band 1 (7458.92), Band 3 (7677.07) and Band 4 (7270.11). The MSEs at 1 bpp for Band 1 (1.90864), Band2 (3.00191) and Band4 (3.6148) are low while it is high for Band 3 (15.3979). Wavelet transform concentrated very less signal power into the finer components at both the resolution levels, 1 and 2 of IRS image.

DWT concentrates similar signal content into subbands of bands 1, 2 and 4, and higher signal content into subbands of Band 3. This behaviour of DWT depends on the filters chosen. Band 3 deviates significantly from Bands 1, 2 and 4 in Wavelet domain. This observation is similar across all the subbands of IRS data. So the PSNR values for Band 3 are poor as compared to other Bands (since KRGSVQ encoding is done in Wavelet domain). This is an interesting observation because Band 3 is similar to Bands 1 and 4 in spatial domain but not in Wavelet domain.

4.2. Landsat TM Six-Band Data

Next we include results of Landsat 4 TM data, we took data of six bands (excluded thermal band) of two regions - one near Lisbon, Portugal and the other near Central Washington, DC. These two data-sets have been used by many researchers in the past, so we considered these data-sets for comparing the results.

For Washington area, LH_2 and HL_2 contain almost the

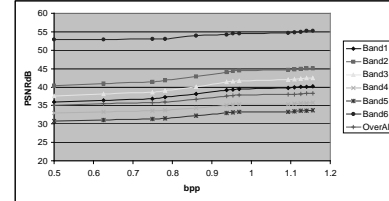


Figure 4: PSNR versus bpp for Landsat image of Washington, DC area.

9 bpp	1 bpp $N_g = 9$ $N_i = 7$ Size 2×2	0.5 bpp $N_g = 47$ $N_i = 209$ Size 4×4
1 bpp $N_g = 7$ $N_i = 9$ Size 2×2	0.5 bpp $N_g = 93$ $N_i = 163$ Size 4×4	0.5 bpp $N_g = 30$ $N_i = 226$ Size 4×4
0.5 bpp $N_g = 39$ $N_i = 217$ Size 4×4	0.5 bpp $N_g = 39$ $N_i = 217$ Size 4×4	0.5 bpp $N_g = 39$ $N_i = 217$ Size 4×4

Figure 5: Sub-band bit allocation for GER image of an area near Rhine, Germany at 1.094 bpp.

same signal power and hence are allotted 1.5 bpp each, while HH_2 contains significant signal and is assigned 0.5 bpp. HH_1 is discarded for Washington area but allotted 0.5 bpp for Lisbon data. Figure 4 represents PSNR versus bits per pixel for this data set, almost similar is the shape of the plots of Lisbon area. All the plots have very marginal slope, this indicates that PSNR does not vary much within a bpp range.

4.3. Hyperspectral Data

We use hyperspectral data acquired by two sensors - GER and AVIRIS, see [6] and [20] respectively for details of the datasets. Bit-allocation for GER data (bands 14 - 17) is included in Figure 5. For this data, HH_1 contains some information and 0.5 bpp is allotted. Bands 14 - 17 of GER data are quite similar in both spatial and DWT domains. Hence, all the four bands have almost the same signal power and identical high PSNR values, the PSNR vs. bpp plots are identical.

4.4. Comparison with Others

In Figures 3 and 4, the slope of the PSNR versus bpp is not significant while reducing the sizes of shape and gain codebooks within a range of bpp. This is an important advantage of this technique with KRGSVQ on wavelet coefficients rather than on image domain - see [6], their technique resulted in a greater slope of the curve. Secondly, slope of the plots of PSNR vs. bpp is almost equal for all bands which also indicates that the technique is independent of the band power. We found this behavior across the images taken from different sensors. This proves our

assumption, and also the shape invariance assumption of KRGSVQ; these assumptions are made use in KRGSVQ encoding coupled with Generalized BFOS for optimal bit-rate allocation. This phenomenon gives us a stable bit-rate.

Hyperspectral data and most of the bands of multispectral data are quite identical in DWT domain, and are encoded well with our technique. Among the recent work, 3-D DWT technique works for hyperspectral but not for multispectral data, [19] and [20]. We also include here a few of the PSNR/SNR results for comparison at 0.14 bit/pixel/band. Our technique resulted in SNR of 21.96 dB while it was 20.6 dB for Landsat image of Lisbon area by Gelli and Poggi's technique [11]. The PSNR obtained with our technique was 36.69 dB for Washington area while VBS and FBS [14] gave 36.04 dB and 36.48 dB respectively. Other results will be presented during the conference.

5. Conclusions

In this paper, we developed a compression technique for multispectral and hyperspectral data using wavelet transform. The wavelet coefficients are quantized using KRGSVQ and encoded using Generalized BFOS algorithm for optimal bit-allocation. We made an assumption that spectral correlation exists in the biorthogonal subclasses of such data, the assumption was shown to hold good by the obtained results. Bands of multispectral data respond differently to DWT. The bands which are similar in Wavelet domain are encoded extremely well, this is confirmed by the results obtained using this technique. This technique is shown to work across both multispectral and hyperspectral data. We compared the numerical results obtained with our technique with some of the recently proposed techniques and got superior results.

To analytically validate the hypothesis that spectral correlation exists in biorthogonal subclasses of multispectral and hyperspectral data, is an area of further investigation.

References

- [1] G. P. Abousleman, M. W. Marcellin, and B. R. Hunt. Compression of Hyperspectral Imagery Using the 3-D DCT and Hybrid DPCM/DCT. *IEEE Transactions on Geoscience and Remote Sensing*, 33(1):26 – 34, January 1995.
- [2] F. Amato, C. Galdi, and G. Poggi. Embedded Zerotree Wavelet Coding of Multispectral Images. In *IEEE International Conference on Image Processing*, volume 1, pages 612 – 615, October 1997.
- [3] M. Antonini, M. Barlaud, P. Mathieu, and I. Daubechies. Image Coding using Wavelet Transform. *IEEE Transactions on Image Processing*, 1:205 – 220, April 1992.
- [4] R. L. Baker and Y. T. Tse. Compression of High Spectral Resolution Imagery. In *Proc. SPIE*, volume 974, pages 255 – 264, 1988.
- [5] L. Breiman, J. H. Friedman, R. A. Olshen, and C. J. Stone. *Classification and Regression Trees*. Wadsworth, 1984.
- [6] G. R. Canta and G. Poggi. Kronecker-Product Gain-Shape Vector Quantization for Multispectral and Hyperspectral Image Coding. *IEEE Transactions on Image Processing*, 7(5):668 – 678, May 1998.
- [7] P. A. Chou, T. Lookabaugh, and R. M. Gray. Optimal Pruning with Applications to Tree-Structured Source Coding and Modeling. *IEEE Transactions on Information Theory*, 35:299 – 315, March 1989.
- [8] R. O. Duda, D. G. Stork, and P. E. Hart. *Pattern Classification and Scene Analysis Part 1: Pattern Classification*. John Wiley, 2000.
- [9] B. R. Epstein, R. Hingorni, J. M. Shapiro, and M. Czigler. Multispectral KLT-Wavelet Data Compression for Landsat Thematic Mapper Images. In *Proc. Data Conference Conference*, pages 200 – 208, April 1992.
- [10] B. Furht, S. W. Smolar, and H. Zhang. *Video and Image Processing in Multimedia Systems*. Kluwer, 1996.
- [11] G. Gelli and G. Poggi. Compression of Multispectral Images by Spectral Classification and Transform Coding. *IEEE Transactions on Image Processing*, 8(4):476 – 489, April 1999.
- [12] A. Gersho and R. M. Gray. *Vector Quantization and Signal Compression*. Kluwer, 1992.
- [13] S. Gupta and A. Gersho. Feature Predictive Vector Quantization of Multispectral Images. *IEEE Transactions on Geoscience and Remote Sensing*, 30(3):491 – 501, May 1992.
- [14] J. Lee. Optimized Quadtree for Karhunen-Loeve Transform in Multispectral Image Coding. *IEEE Transactions on Image Processing*, 8(4):453 – 461, April 1999.
- [15] S. G. Mallat. A Theory for Multiresolution Signal Decomposition: The Wavelet Representation. *IEEE Transactions on Pattern Analysis and Machine Intelligence*, 11(7):674 – 693, July 1989.
- [16] E. A. Riskin. Optimum Bit Allocation via the Generalized BFOS Algorithm. *IEEE Transactions on Information Theory*, 47:400 – 402, 1991.
- [17] M. J. Sabin and R. M. Gray. Product Code Vector Quantizers for Waveform and Voice Coding. *IEEE Transaction on Acoustics, Speech and Signal Processing*, 32(3):474 – 488, June 1984.
- [18] J. A. Saghi and A. G. Tescher. Near Lossless Bandwidth Compression for Radiometric data. *Optical Engineering*, 30:934 – 939, July 1991.
- [19] Y. H. Tseng. Hyperspectral Image Compression Using Three-Dimensional Wavelet Transformation. Personal Communication, June 2002.
- [20] Y. H. Tseng, H. K. Shih, and P. H. Hsu. Hyperspectral Image Compression Using Three-Dimensional Wavelet Transformation. *Asian Journal of Geoinformatics*, 2002.
- [21] J. Vaisey, M. Barlaud, and M. Antonini. Multispectral Image Coding Using Lattice VQ and the Wavelet Transform. In *IEEE International Conference on Image Processing*, pages 712 – 716, 1998.
- [22] P. H. Westerink, J. Biemond, and D. E. Boekee. An Optimal Bit Allocation Algorithm for Sub-band Coding. In *IEEE International Conference on Acoustics, Speech and Signal Processing*, pages 757 – 760, 1988.